ABSTRACT

Title of Document: MODELING POWER CONSUMPTION AND OPERATION IN A BISTABLE ELECTROWETTING-BASED DISPLAY

Trinish Chatterjee, Nazifa Chowdhury, Jason Ittner, Alexander Jiao, David Nguyen, Karam Singh, Alexander Weatherford

Directed by: Dr. Pamela Abshire

Institute for Systems Research

Team VOLTAGE is an undergraduate research team based in University of Maryland's Gemstone research program. Their objective is to advance research related to modeling e-paper technologies. Experimentation with electrowetting display fabrication techniques, followed by modeling based on measured parameters is performed. Both numerical and circuit-based simulations are performed. Numerical simulations demonstrate correlations between pixel size, alpha constant, actuation voltage, and power consumption. Circuit-based simulations demonstrate a method for determining power consumption of an electrowetting-based display and give an accurate power consumption for a specified display.

MODELING POWER CONSUMPTION AND OPERATION IN A BISTABLE, ELECTROWETTING-BASED DISPLAY

By

Team VOLTAGE

Trinish Chatterjee

Nazifa Chowdhury

Jason Ittner

Alexander Jiao

David Nguyen

Karam Singh

Alexander Weatherford

Thesis submitted in partial fulfillment of the requirements of the Gemstone Program

University of Maryland, College Park

2019

Advisory Committee:

Dr. Pamela Abshire, Mentor

Dr. Sangwook Chu, Discussant

John Abrahams, Discussant

Dr. Gradimir Georgevich, Discussant

Dr. Matthew Hagedon, Discussant

Acknowledgements

We would like to thank the numerous individuals who contributed to our research. Thank you to each of our Launch UMD donors, listed below.

We would also like to thank the many researchers who aided us in our experiments: Dr. Kristin Charipar and the Naval Research Laboratory, Dr. Matthew Hagedon and the Johns Hopkins Applied Physics Lab, and the University of Maryland FabLab, especially John Abrahams.

We are incredibly grateful for the support of our mentor, Dr. Pamela Abshire. We would also like to thank Dr. Sangwook Chu for his generous guidance and for permitting our use of his equipment.

Finally, we thank the Gemstone staff and the Gemstone community for their unwavering friendship and support.

Launch UMD Donors

Wenjie Jiao, Dr. Pamela Abshire, Luis Montes, Achint Kaur, John Hallock, Kowsar Chowdhury, Shahid Chowdhury, Sherry Hsieh, Manaahil Rao, Tania Chatterjee, Gregory Capasso, Michael Tao, Anthony Ostuni, Lauren Fischer, Timothy Chen, Zubair Khan, Carlos Gonzalez, Nathaniel Renegar, Paige Chan, Paul Hallock, Kevin Nguyen, Bishwanath Chatterjee, Stacey Pridgen, Lara Fu, Team ART, Emily Yang, Adam Elaoud, Erin Murphy, Janet Sun, Morgan Janes, Johan Vandegriff, Emily Dao, Justin Pan, Allison Chen, Rex Ledesma, Jessica Kang, Michael Anderjaska, Lisa Rishell, Chris Nakamura, & Mary Robichaux.

Table of Contents

Introduction

The electrowetting phenomenon can be used to create large, low-power displays that would be superior to current display technologies. Electrowetting-based displays (EWDs) have demonstrated superiority to current display technology in many ways [1]. High reflectivity, low power usage, and potential flexibility make them an excellent candidate for paper-like electronic displays [2] [3]. In addition, EWDs can be bistable, allowing for significantly reduced power usage during operation [4] [5].

Our model consists of numerical simulations and a high-level overview of circuit systems which leverage passive matrixing and bistability to characterize an EWD. Electrical properties of the display are determined using CircuitLab and MATLAB simulations of the system that effectively model switching speed and energy consumption.

Literature Review

Electrowetting

Electrowetting refers to the change in the "wettability" of a surface when a voltage is applied to that surface. Wettability is the ability of liquids to stay in contact with a surface, and is usually quantitatively measured using the apparent contact angle between the droplet and the surface [6]. When a voltage is applied to a surface and a small droplet, the contact angle of the droplet can change, causing the it to contract or spread out, as shown in Figure 1(a). This only happens substantially for droplets with diameters of 1 mm or less, and is described mathematically by the Lippmann-Young equation:

$$\cos\theta(V) = \cos\theta_0 + \frac{\varepsilon V^2}{2\gamma_{\mathrm{LV}} d}$$

In this equation, the apparent contact angle θ_0 changes as a function of the dielectric constant of the surface (ε), the applied voltage (V), the thickness of the dielectric surface (d), and the surface tension between the droplet and the air (γ_{LV}) [7]. The contact angle between a droplet and the surface, without an external electric field is determined predominately by surface tension and not by gravity, as it would be for larger droplets. The surface tension of the boundaries between the surface, the liquid, and the other medium are defined by their Gibbs Free energy, which has both chemical and electrical components. Surface tension is also a measure of interfacial force per area, which determines the curvature of the droplet. By putting an external electric field in the system, the Gibbs Free Energy is manipulated, causing a change in surface tension and

thus a change in the droplet's shape. A significant change in the droplet's shape can even be used to move the droplet across electrodes given the droplet's small size. In practice, aqueous salt solutions are often used as the fluid droplets, and the microfluidic droplets can be exposed in air or immersed in other mediums such as oil.

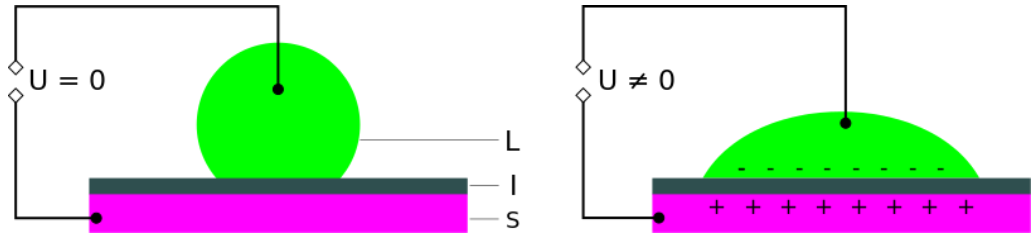

(1a)

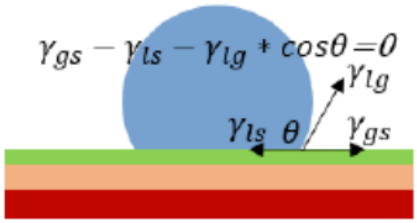

(1b)

Figure 1. (a) The concept of electrowetting. The green droplet changes its shape and contact angle with the surface upon the application of voltage through the system. Image taken from [8]. (b) The interfacial tensions in an electrowetted droplet. Image taken from [9].

Electrowetting-based displays are built with each pixel containing a droplet on a hydrophobic surface. The fluid is naturally repelled by the hydrophobic surface. When a voltage is applied to the surface, the droplet reforms. Droplet manipulation is one of the most fundamental applications of electrowetting. The transport of droplets between electrodes occurs as a result of uneven interfacial surface tensions. A potential difference between electrodes that are covered by hydrophobic and capacitive layers which creates

an imbalance in pressure across the droplet thus allowing for bulk fluid movement [10]. The hydrophobic layer of an electrowetting device ensures that the droplets of ink or oil do not stick to the dielectric layer allowing the droplet to be free to spread out on the surface without obstructions when voltage is applied [11].

Electrowetting-based Bistable Displays

Electrowetting displays (EWDs) have exhibited impressive characteristics across a variety of studies [12] [13] [14] in spite of their current limitations, thus demonstrating promising potential to replace existing displays.

Bistable displays, which are displays that do not require the constant reapplication of voltage to maintain state, show promise in the building of large-scale, low power displays like billboards or e-wallpaper. There are many forms of bistable displays, but we will focus on simulating the structure proposed by [4]. This display offers benefits in ease-of-manufacturing as well as the potential for color. In the "on" state, this display uses the surface tension of oil to keep the raised pixel structure covered, thereby reflecting no light. In the "off" state, the oil is kept pinned in channels by gravity, thereby creating a bistable effect where power only needs to be applied to change the state of a pixel. When a potential difference is applied, the saline solution moves in response, pushing the oil to its stable resting state [15].

Electrophoretic Displays (EPDs) like those found in the Amazon Kindle are also bistable, but they have difficulties with multiple colors and video-speed refresh rates. Because they do not have those limitations, we focus exclusively on bistable EWDs.

Matrixing

Pixel addressing in modern displays is often achieved via either passive or active matrixing [16]. Passive matrix schemes use a grid to supply charge to a pixel on the display. The rows and columns are individually actuated to toggle a pixel on the intersection point of the display. To turn on a pixel, the controlling circuit applies a voltage on the correct column of one substrate and a ground on the correct row of the other. The row and column intersect at the designated pixel, which delivers voltage to manipulate the pixel. While this matrixing scheme requires fewer connections, it's less power efficient and often leads to slower switching speeds [16].

Active matrix schemes generally use Thin Film Transistors (TFTs) as well as capacitors to more selectively address select pixels. To address a pixel, a voltage is applied to the proper row and then a current is applied to the corresponding column. A capacitor located on the pixel can hold the charge until the next refresh cycle, which stores the state of selected pixel groups while other pixels are updated [17]. This scheme naturally results in faster switching speeds at the cost of increased complexity and a greater number of connections.

Passive and active matrixing represent the two predominant modes for pixel addressing in display technologies. Whereas most LCD displays utilize active matrixing, we have chosen to use passive matrixing in the proposed display model for its simple structure that lends itself to bistable displays.

Simulations and Modeling

The EWD pixel lumped-circuit consists of modeling each element of the pixel as a parallel capacitor-resistor combination in series with adjacent elements. The capacitance and resistance of a material can be determined by converting from the resistivity and capacitance of the materials in the physical display. This accurately models the charging and switching behavior of the pixel and allows for power consumption simulations. Modeling can be done with various circuit simulators such as CircuitLab or PSpice. By creating a simplified model for a display, one can extract various features for the displays and can integrate on the design in an informed process.

Existing Displays

Liquid Crystal Displays

Smartphones, laptop screens, and electronic wearable devices all predominately use LCD screens. Though variations exist, all LCDs have two major components: the LCD panel in front and the backlight behind it. The LCD panel filters light from the backlight to the desired brightness for every pixel by allowing less or more light to pass through the panel [18]. To produce color, the pixels use RGB segmentation to filter the light, which intrinsically loses about 2/3 of the actual light emitted by the backlight [19]. This naturally necessitates a high backlight intensity to power even simple screens. Researchers have determined that the power consumption from LCDs is a linear function of the backlight intensity [18]. That is, the more intense the backlight—and therefore the brighter the screen is—the more power that is consumed by the display.

Electrophoretic Displays

Electrophoretic display (EPD) technology is the most widely-used, low-power, paper-like display technology currently available on the market, commonly used by e-readers such as the Amazon Kindle [20]. The technology is based on electrophoresis, the phenomenon by which an applied electric field rearranges charged pigment particles in a colloidal suspension. This suspension is often referred to as "e-ink" colloquially. The rearrangement of charged pigments is what forms images for display purposes [21].

Organic Light Emitting Diodes (OLEDs)

Organic Light Emitting Diodes (OLEDs) are a relatively new but increasingly popular display technology. OLEDs are like LEDs in that they are diodes which emit light when current passes through; however, OLEDs are created by placing organic carbon-based materials between two conducting plates [22].

Power Consumption in Existing Displays

Existing displays use a variety of underlying technologies. LCDs are the most ubiquitous, but the required backlight requires significant power. LED displays are LED-backlit LCDs, the successors to CFFL-backlit LCDs. OLEDs are not LCDs; they are emissive and do not need a backlight. OLEDs enable thinner displays and without the wasted thermal energy of a backlight. OLED displays are more expensive, but they are expected to continue growing in popularity [23], [24].

MicroLED technology gained widespread attention in 2018 when Samsung showcased a prototype 146" display [25]. MicroLED has been used for ultra-low-power microscale light sources [26] and may also provide lower power and higher resolution

than LED LCDs [27]. Like OLED, its present competitiveness is limited by manufacturing difficulty, but its promising characteristics may make it a competitive technology in the near future [28]. For our later analysis, we omit comparison to microLED displays due to a lack of openly available power consumption data.

We will use the results of Fernández et al. [29], which defines approximate power densities for various display technologies. The power density in mW/cm^2 provides a standard metric for power consumption per size. Note that "a-Si TFT" refers to an active-matrixed LCD. We refer to this figure in our results section.

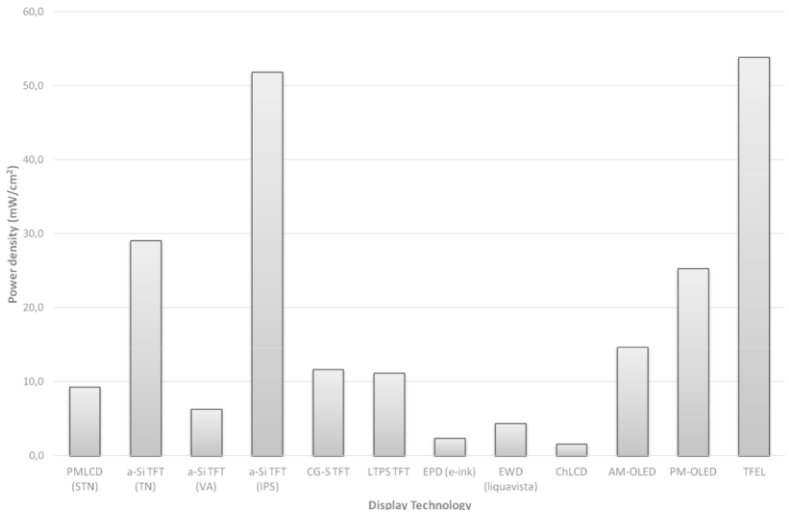

Figure 2: Power Density by Display Technology, taken from [29]

Methodology

Introduction

We developed a circuit model for a low-cost, low-pixel-density, scalable electrowetting-based digital display that is viable for large, consumer displays. Concurrently, we hoped to test the parameters of this model by fabricating and performing measurements on single aspects of an EWD.

Our research started with the testing of various materials and designs in prototypes with the intent to refine minimally-viable electrowetting-based display components. We then used results from these experiments as well as empirical evidence from our research to select, design, and record the basic elements of a final EWD. These elements could then be used to justify the results from a circuit model and qualify the final design we simulate. The design we chose to model would have a multitude of potential applications wherever low cost and low power consumption are more essential than high resolution.

Initial Experimentation

Our original methodology was centered around varying the materials and fabrication processes for the functional layers of a display. By doing this we intended to discover new combinations of low-cost materials and fabrication methods for producing functional electrowetting-based displays. This process included attempts to test and 3D print simple pixel structures. Unfortunately, due to budget constraints, we were unable to obtain access to a 3D printer with fine enough resolution to print pixel structures capable of electrowetting.

We also attempted replication of the copper sheet droplet transport through copper etching seen by Abdelgawad et al [10]. Copper etching is a method in which we lay ink onto a copper sheet, dip it into an etchant, and then wipe away the ink to reveal a conductive layer on which we can transport water particles via electrowetting. This is a relatively cheap method of fabrication and one of the first that we tried. Ink was deposited with a laser ink jet printer before dipping the sheet into the etchant. Then a layer of plastic wrap was placed as the dielectric, followed by Rain-X as the hydrophobic layer. The result of this experimentation is shown in Figure 2. This model did not successfully transport droplets although we did see movement of the water. There were too many control variables and the fabrication methods were too imprecise to determine specific areas of improvement. We then decided to try more robust methods of EWD fabrication.

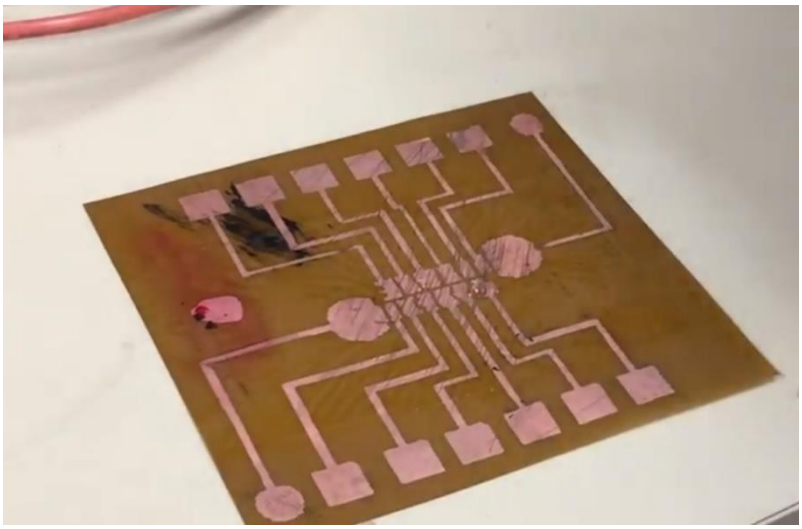

Figure 3: Replication of the copper-etched droplet transport design.

Final Design Selection

We decided to test different materials and fabrication techniques in order to find an optimal display design for low-cost and low-power displays. Research into EWDs yielded several potential low-power, bistable designs that could be simulated. We settled on a design by Charipar et al. [4]. which was chosen for its bistable design and relatively simple construction. Construction of this display was more difficult than expected, which made iteratively trying new materials unfeasible. Consequently, we decided to simulate and model aspects of the display to measure power consumption.

The Charipar et al. [4] design featured a pixel stack which included a lower level of etched ITO to allow for pixel actuation, a pixel structure which allows for a dyed oil to be concealed or revealed, and a top-level electrode for passive matrix control.

The basic operation of a single pixel is shown in Figure 3. The bottom layer is ITO coated glass which acts as a control electrode. On top of this, a layer of SU-8 is used as both a dielectric and a pixel structure and Fluoropel is used as the hydrophobic layer. Dyed dodecane oil sits on top of the SU-8 and saline water fills the space between the oil and the top electrode. The top electrode composed of ITO coated glass provides a system ground. The resting state of the oil is on the raised SU-8 channel and when an actuation voltage is applied to either the pixel electrode on the bottom, it moves to the channel, the second resting state. Since the oil is dyed dodecane, the reflectivity of the pixel changes drastically based on the position of the oil, thereby creating an on/off effect. The oil moves in response to the bulk movement of saline that is induced by the potential difference between channel electrodes.

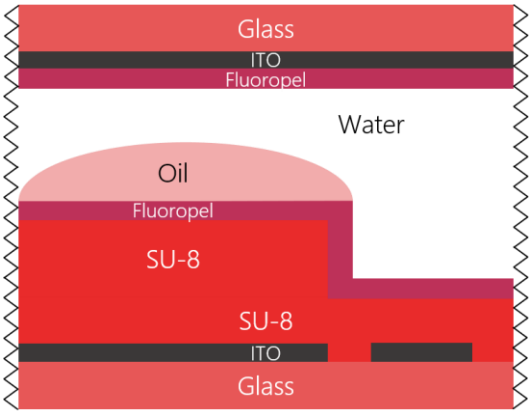

Figure 4: Basic stack construction based on Charipar et al. design

The bottom electrode pattern is shown below in Figure 4. There are two electrically separate patterns for each row - the pixel and channel patterns. The voltage level at these patterns is independent and appropriately actuated when a change of state is needed. A high voltage at the pixel electrode and low voltage at channel causes the oil to move from on top the pixel into the channel and vice versa. The pixels were 300×900 µm and channels were 100x900 µm. The dielectric SU-8 was 3 µm, and the pixel SU-8 was 22 µm. The total thickness of the device built in [4] was 250 µm.

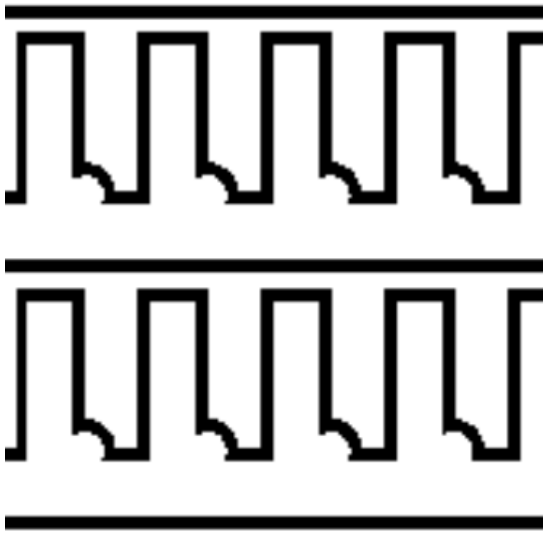

Figure 5: Electrode pattern of Charipar et al. design.

The display structures were fabricated using spin coated SU-8 and photolithographic etching. ITO electrodes were fabricated using HCl etching. The masks used for etching both ITO and the SU-8 are shown below (see Fabrication Techniques for more detail). The electrode masks were specifically designed to allow for a passive matrixing scheme (see Control Mechanisms below). Masks were designed in Adobe Illustrator and printed on clear plastic.

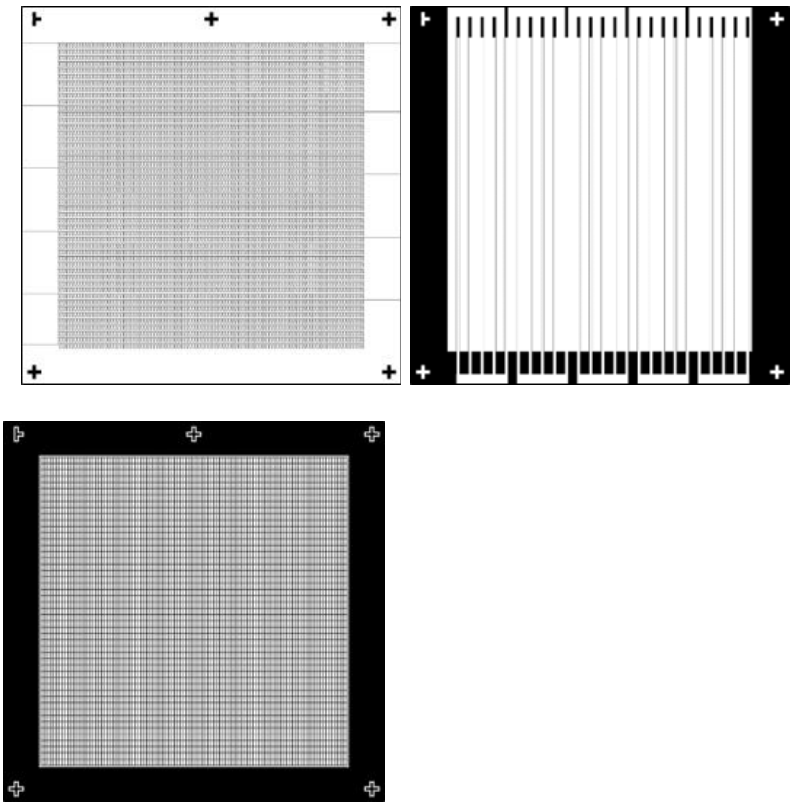

Figure 6: Masks for bottom electrodes (left), top electrodes (center), and pixel structure (right).

Control Mechanisms

As noted previously, passive matrixing can be enabled in a display by dividing the bottom substrate into rows and the top substrate into columns. Applying a voltage to the appropriate row and a ground to the appropriate column will actuate the pixel located at the intersection of the row and column. To prevent the actuation of other pixels, a set voltage, which can be determined empirically, can be applied to the remaining rows. This guarantees that the voltage difference across the remaining rows never exceeds that of the actuation voltage, ensuring the pixels do not actuate as seen in Figure 6. In addition to being able to actuate individual pixels, the pixel state is independent of the past pixel states. In order to uncover the pixel structure, a voltage should be applied to the pixel bodies in the row. In order to cover the pixel structure, a voltage should be applied to the pixel channels in the row.

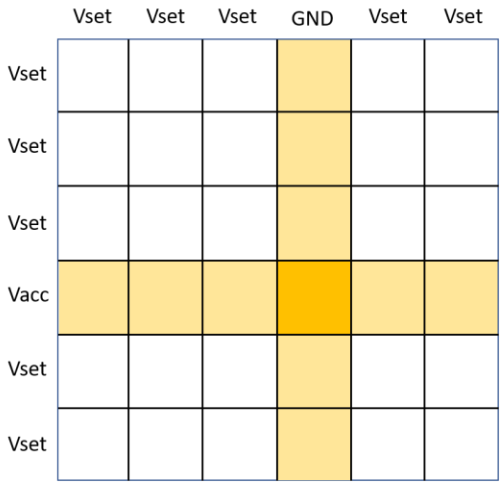

Figure 7: A simplification of the methods used to actuate individual pixels.

To enable preliminary testing of a passive matrixed display, we created ITO masks which would be used to create 25 ‘pixel blocks’, each controlling a subset of

individual pixels. By doing this, we would ensure that individual pixel failure did not adversely affect the quality of the display while testing pixel indexing through the 'pixel blocks'. In addition to being largely unaffected by individual pixel failure, the pixel block setup would allow us to note the frequency and duration of pixel failure. To allow us to actuate pixels unidirectionally, we connected all channel rows in the leftmost section of the mask and all pixel body rows on the right most side of the mask. The masks used can be referenced in Figure 5. By applying the same scheme described above, we would be able to actuate a single pixel at a time, fully taking advantage of the bistability of the display in practice.

Fabrication Techniques

Many precise steps are required to create samples of high enough quality to be tested. We have not completed all fabrication steps required for a fully functional display, but only those required to test the wetting performance. Some testing was completed with un-patterned ITO, but we have since patterned it; this choice provides a more realistic sample for testing and enables more involved future testing.

ITO Patterning

Following design of the masks shown in Figure 5, the top and bottom electrodes were etched first. Glass samples plated with 185 nm ITO [30] were used for both top and bottom electrodes. First, a layer of HDMS and then a layer of S1813 [31] are applied via spin-coating. Then, each sample is baked at 100 °C for 1 minute. A mask aligner is then used to expose the pattern into the S1813. Then the samples are soaked in S1813 developer to remove unwanted photoresist. After this, the samples are soaked in 37%

HCl for 12 minutes with agitation to remove ITO. The remaining S1813 [15] is then removed and glass plates coated in patterned ITO remain.

We had considerable issues with exposure and etching times. Figures 7 and 8 are a few examples. The samples appear pink where ITO was etched before the photoresist is removed. We were not able to remove ITO uniformly, even with agitation; ITO was removed faster from the center of the samples than from the edges. We attempted to combat this by "side-etching", treating and agitating just the sides of the samples in HCl, but we struggled to do this with accuracy without compromising the pattern. The required etching time is dependent on the exposure. Initial attempts exposed for 210uJ/cm^2, but a higher exposure of 360mJ/cm^2 allowed for better samples.

Figure 8: At left, pixel channels are under-etched, possibly a result of underexposing the pattern. At right, an etch line did not reach the edge of the device. ITO removed (pink) from edge did not reach the regional boundary.

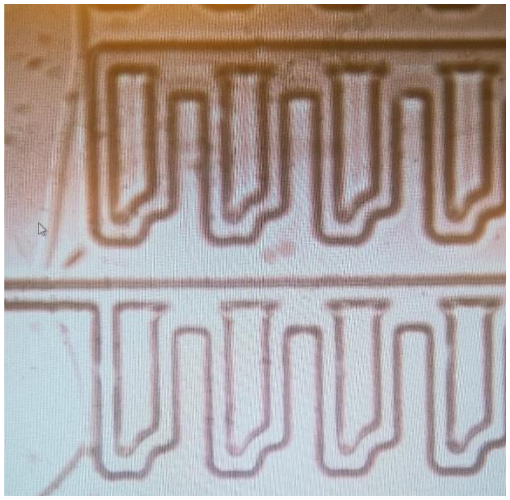

Figure 9: Over-etched patterns bottom electrode pattern.

Each ITO-etched sample was electrically tested with a multimeter. Acceptable ITO etches had resistance of less than or equal 300Ω between channels and channel contacts and between pixels and pixel contacts. Between regions which should be electrically disconnected, resistances were required to appear as an overload on the multimeter. Samples were considered acceptable as long as no more than two adjacent regions were electrically connected.

SU-8 Deposition

We used four varieties of SU-8 which each have different recipes. The SU-8 is deposited with a spin coater as well. Per the SU-8 3000 datasheet [32], both SU-8 3005 and 3035 were spun for 10s at 500 rpm and 30s at 4000 rpm. Per the SU-8 3000 datasheet [32], both SU-8 3005 and 3035 were spun for 10s at 500 rpm and 30s at 4000 rpm. Per the SU-8 3000 datasheet [32], both SU-8 3005 and 3035 were spun for 10s at 500 rpm and 30s at 4000 rpm. 3005 was soft-baked for 2 minutes at 95°C, while 3035 was soft-baked for 10 minutes. 3005 was exposed with 225 mJ/cm^2 and post-baked 1 minute at 120°C. 3035 was exposed with 300 mJ/cm^2 and post-baked 3 minutes at 120°C.

Per the SU-8 2000 datasheet [33], SU-8 2005 was spun at 500 rpm for 10s with an acceleration of 100 rpm/s then 4500 rpm for 30s with 300rpm/s acceleration to achieve a thickness of approximately 4.5µm. Per the SU-8 2000 datasheet [33], SU-8 2005 was spun at 500 rpm for 10s with an acceleration of 100 rpm/s then 4500 rpm for 30s with 300rpm/s acceleration to achieve a thickness of approximately 4.5µm. Per the SU-8 2000 datasheet [33], SU-8 2005 was spun at 500 rpm for 10s with an acceleration of 100 rpm/s then 4500 rpm for 30s with 300rpm/s acceleration to achieve a thickness of approximately 4.5µm. Per the SU-8 2000 datasheet [33], SU-8 2005 was spun at 500 rpm for 10s with an acceleration of 100 rpm/s then 4500 rpm for 30s with 300rpm/s acceleration to achieve a thickness of approximately 4.5µm.

Samples were then soft-baked for 3.5 min at 95°C, exposed with 135mJ/cm^2, and post-baked at 120°C for 2 minutes. SU-8 2010 was spun at 1000 rpm, soft-baked for 3.5 min at 120°C, exposed with 218mJ/cm^2, and post-baked for 4.5 minutes at 120°C. Each sample was post-baked for 2 minutes at 95 °C. Then the samples were placed in the mask aligner to have the patterns etched, and a post-exposure bake followed at 100°C for 2 minutes, adjusted per SU-8.

Fluoropel Application

After SU-8 deposition, samples are spin-coated or dip-coated in Fluoropel. For Fluoropel PFC1601V, we spin-coat at 2000rpm for 30s, post-bake at 120°C for 15m to achieve approximately 50nm uniform coating. For Fluoropel 800, we dip-coat for 2 minutes and then post-bake for 10 minutes at 120°C.

Simulated Models

To augment our lab research, we performed CircuitLab and MATLAB simulations to obtain a reasonable estimation of power consumption and operational control of the display. [4] reported an estimated power consumption of 63.4 $\mu J/in^2$, however this calculation was obtained with an estimated switching speed of 36ms. This limitation was due to the frame rate of the camera being used to test the device. Circuit models were developed to estimate the display characteristics which were compared against the experimental results of the Charipar et al. We focused specifically on the dark-to-light transition, where the oil begins sitting on top of the pixel area and then vacates into the channel after the application of voltage. Constants for the simulations can be found in Appendix A, and code in Appendix B.

CircuitLab Simulation

A CircuitLab simulation was created to characterize the display proposed by [4] and to do analysis on the individual components. This would allow for a standardized model which could be manipulated to make improvements on the design long term and allow for more robust changes over time. To confirm the quality of the model, the resulting power consumption was compared with the empirical results reported by [4].

The circuit model was based off the lumped resistor-capacitor model used to model the electrical characteristics of different materials [34]. We included the following components: ITO, Saline, Oil, a hydrophobic layer, and the SU-8 dielectrics. The final model was then run, and the total power was calculated by integrating the instantaneous powers over 36ms. This result was then compared with the 63.4 $\mu J/in^2$ reported in [4].

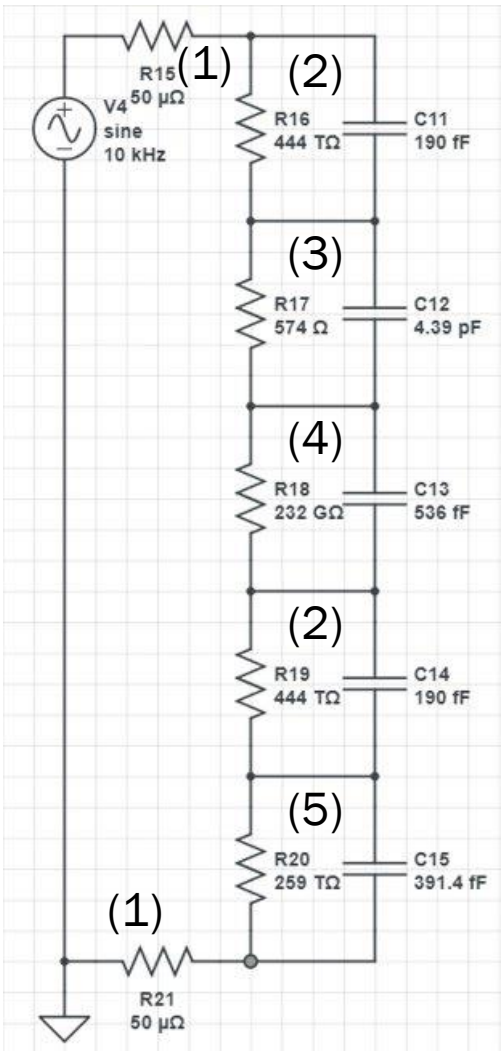

Figure 10: Modeled circuit with components labeled as (1) ITO, (2) Hydrophobic layer (3) Saline, (4) Oil, (5) SU-8.

MATLAB Simulation

We also used a MATLAB simulation to estimate the energy required to switch one pixel based on a differential-equation model. This MATLAB simulation was based off of the model suggested by Tang et al.[35] and Zhao et al. [36] from Guofu Zhao's group at South China Normal University, which suggested that the oil and the pixel could be modeled as two lumped elements with a resistance and a capacitance across the ends

[35]-[36]. This can be seen in the figure below (Figure 1 from [36]), where the hydrophobic layer and the pixel structure is combined into “FP” (fluoropolymer).

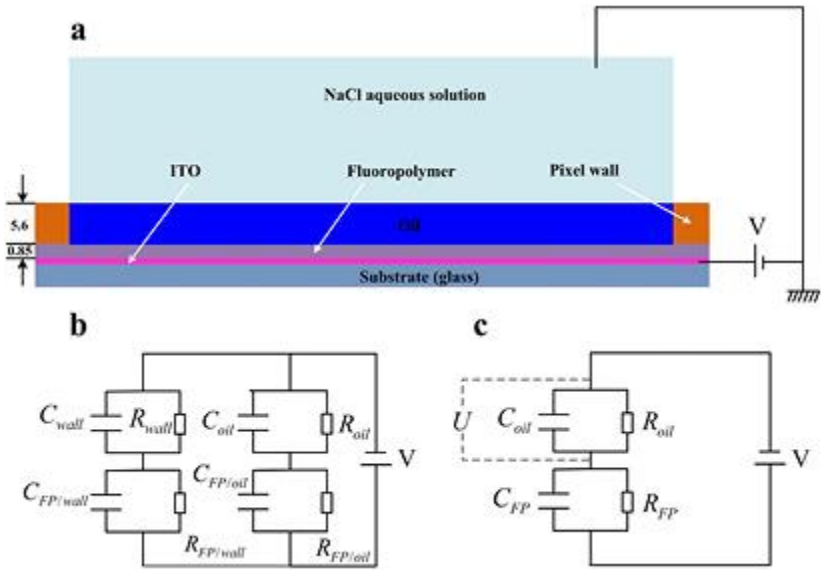

Figure 11. Equivalent circuit model from [18]

This equivalent circuit model ignores the water as well as the hydrophobic layer. The paper also suggested that the circuit could be solved for the voltage across the oil using a basic differential equation derived from the s between circuit elements. The resistances and capacitances are calculated using the formulas associated with these elements, as well as the dielectric and conductive properties of the materials used. The dimensions we used were equivalent to the dimensions used in our masks. For the oil, the height was taken to be what the height would be if we assume that 1) the oil sits completely evenly on the entire surface of the pixel, and that 2) exactly half of the oil from the channels surrounding a pixel is transferred onto the top of the pixel.

This gives the equation:

$$\frac{dU(t)}{dt} = \frac{\frac{V(t)}{R_{FP}} - U(t) * \left(\frac{1}{R_{FP}} + \frac{1}{R_{oil}}\right) + C_{FP} * \frac{dV(t)}{dt}}{C_{oil} + C_{FP}}$$

From this differential equation, we can determine the AC voltage of the oil when applying an AC Voltage to the entire device. The group associated with Zhao suggested that at a certain voltage, the oil ruptures and recedes to the sides of the pixel. In their model, the sides of the pixels had walls to pin the oil. In our model, the oil would be unbarred and vacate the pixel surface into the channels. Their results suggest that, due to this vacancy of the oil, the white area ratio of the pixel surface (covered to uncovered pixel surface) decreases in an exponential fashion.

Unfortunately, our lab work did not advance far enough for us to create a proper measurement of how fast this exponential decay occurs. Due to this, we made a few estimations. Firstly, we assume that the vacancy of the oil is related to the energy that the applied voltage adds to the system. This is because the surface tension of the water-oil boundary is affected by the energy added to the system. The capacitive energy of the system is $\frac{1}{2}CV^2$, and since the capacitance of the system is near constant overall, we chose to make the system as:

$$\frac{dW}{dt} = -\alpha * U(t)^2 * W$$

where W is the White Area Ratio.

The choice of alpha was made as follows. In Charipar et al. [4], it was suggested that the pixels switched in less than 36 ms when an excitation of 80V AC (amplitude) is applied to the device. Additionally, a 4.5:1 contrast ratio is considered a web-standard

ratio for text. We therefore decided to set alpha to such a value that the value of W, the white-area ratio, drops from 1.00 to 0.22 (which is 1 / 4.5) in 36 ms. This is a conservative estimate. This alpha constant roughly represents the hydrophobic layer and/or the quality of the model, since a better model or a better fluoropolymer will help the oil vacate faster, and vice versa.

This model allows us to input various values for the input voltage and frequency, the material constants, and the alpha constant. We can output the time it takes for one switch to be made from dark to light, as well as the energy involved in one switch. The results of these simulations were compared with existing literature and lab trials to determine their accuracy.

Results

Our team has taken a broad exploration of electrowetting displays. Our results extend broadly across simulation and modeling, control, and fabrication. Each facet of our results will be discussed independently, while broader connections and implications will be discussed in the Conclusion.

Fabricated Devices

We have constructed the components essential to testing EWOD performance. Our performance results are later compared with our simulation model and used to improve its real-world accuracy. Refer to our Methodology for fabrication details.

The testing apparatus was made available to us by Dr. Sangwook Chu. The apparatus was centered around a high-speed camera with a side view of a needle filled with 1M NaCl in DI water. A droplet is lowered at the end of the needle to contact with the hydrophobic surface and is subsequently captured by the camera. Unfortunately, due to material and time constraints, we were unable to perform this test an oil droplet submerged in saline, which adversely affects the scope of the results, however the tests do demonstrate reversible electrowetting on a substrate.

Our initial wetting tests used samples with un-patterned ITO, a 5-6 μm layer of SU-8 3005, and a thin layer (~50nm) of Fluoropel PFC1601V. The droplet was held over the hydrophobic surface and a 5V peak-to-peak voltage, about 1.8V, at 1kHz was applied. The droplet actuated from rest on the needle to contact with the surface within 20ms and returned to its original shape within 10ms. This first round of testing was limited by our inability to generate large voltages to achieve full wetting.

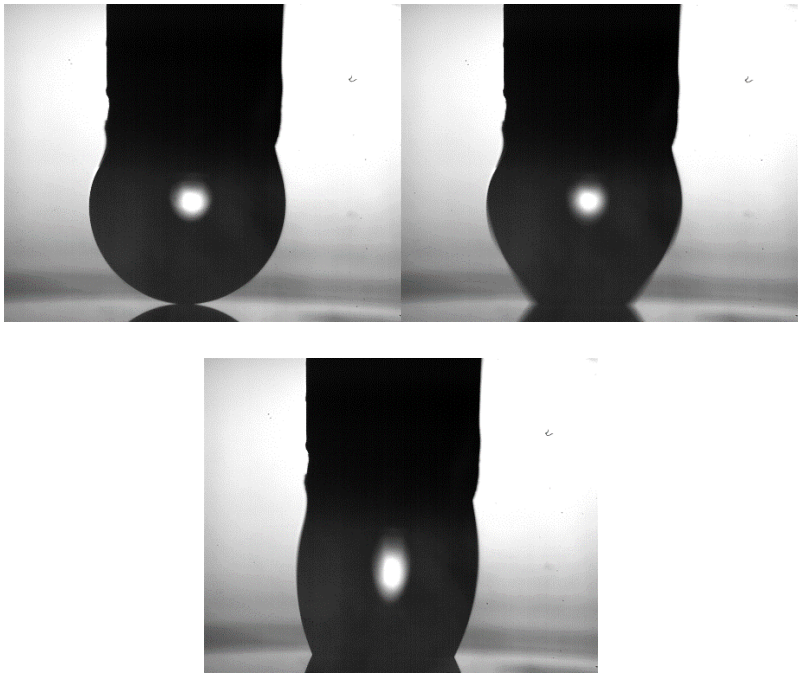

Figure 11: Droplet actuation after application of 5Vpp. Each frame is about 10ms apart.

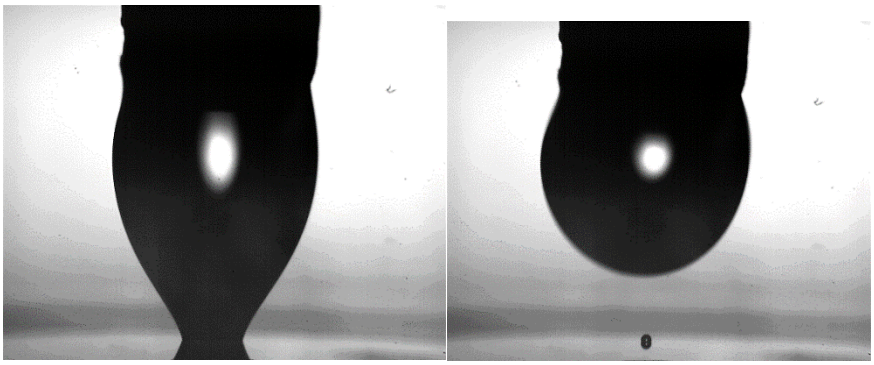

Figure 12: The droplet returns to its original shape after the signal is turned off within 10ms.

The second set of tested sampled were composed of patterned ITO, a 4.5 µm layer of SU-8 2005, and a thin layer of Fluoropel 800. In these trials, we used a step-up boost converter to output 96VDC, 200VDC, 260VDC, and 96VAC, as measured by our

multimeter. The droplet did not respond to 96VDC, responded only slightly to 200VDC, and dielectric breakdown appeared to occur at 260VDC.

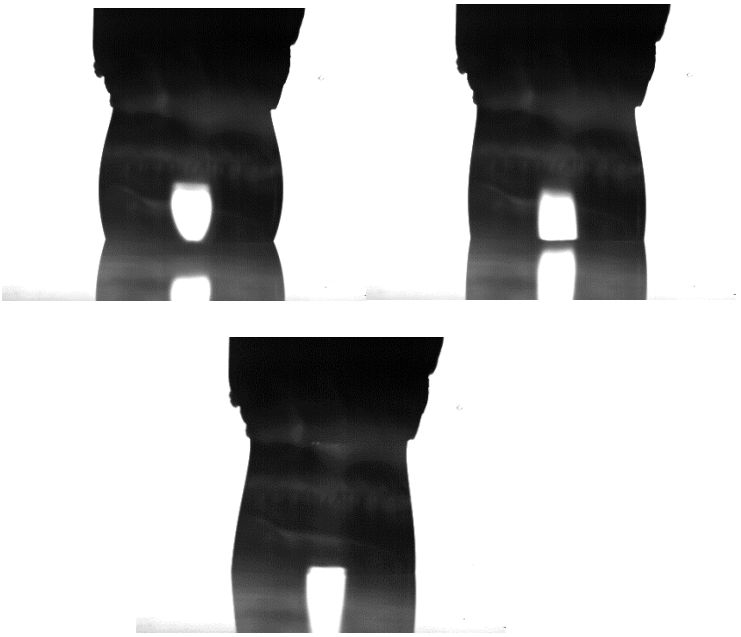

Figure 13: Left to right, pixel shape in response to DC voltages of 96V, 200V, and 260V.

Like in our first round of testing, the droplet responded positively to 96VAC.

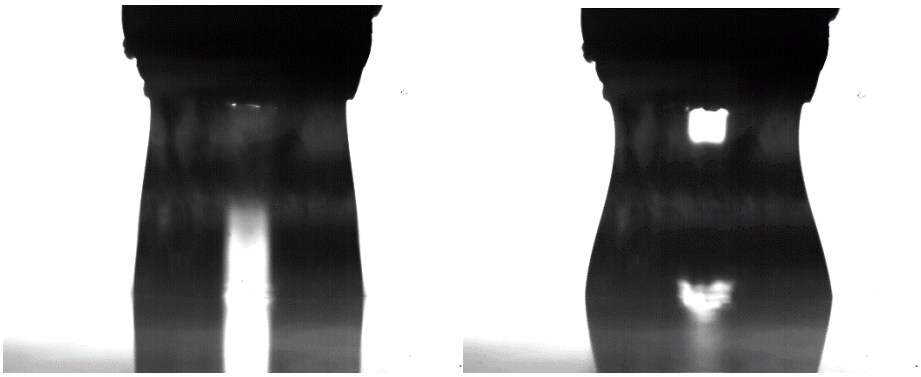

Figure 14: A droplet wets under applied 96VAC in under 10ms.

The team has produced more than 50 samples through our lab work, but many of them were failures or not of high quality. Many of these failures are to be expected for those new to the field. Common failures included over-etching of ITO, failing to evenly deposit SU-8, and misaligning masks.

CircuitLab Model Results

As noted in the methodology, the CircuitLab model was used to generate a baseline model which can be used to do in depth analysis on the display design proposed by Charipar et al [4]. This model could be iteratively improved to simulate more accurate features of the display.

The lumped-circuit model used includes the considers the power consumption of the two ITO layers, the Saline solution, two hydrophobic layers, and the SU-8 dielectric, and is run with a voltage source of 80V AC at 10kHz for 36 ms. Figure 14 displays the model. Constants for the simulations can be found in Appendix A. These constants were determined with respect to a single 900um x 300um pixel, so the results were converted to be reported with respect to inches for ease of comparison.

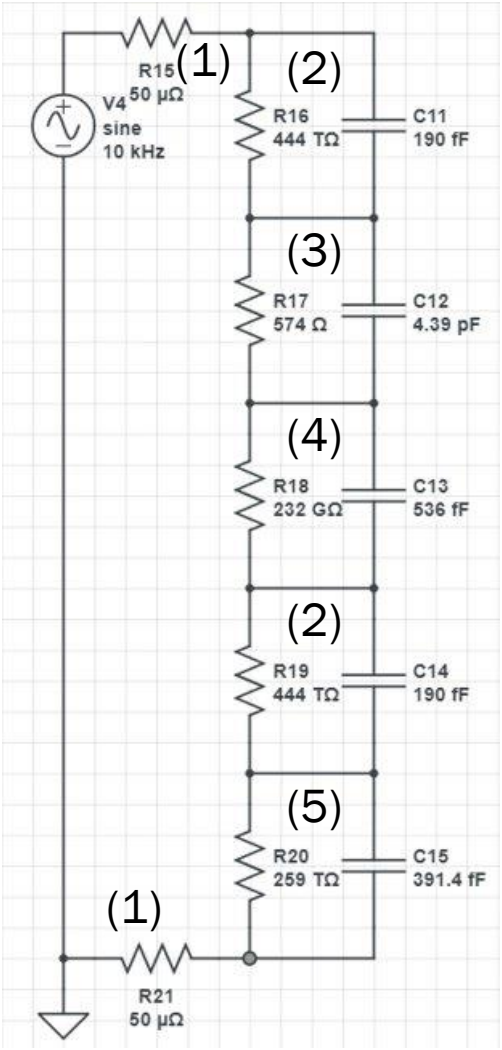

Figure 15. Lumped circuit model of an EWD pixel designed in CircuitLab labeled as: (1) ITO, (2) Hydrophobic layer (3) Saline, (4) Oil, (5) SU-8

Once simulated, the voltage and current at the voltage source were recorded and used to determine the instantaneous power at all data points provided by the simulation. The value of the instantaneous power was subsequently integrated over time for 36ms (reported switching speed), and the resulting value was compared to the reported values. The final power consumption was 3.32×10^{-7} J/pixel in switch, or 7.9×10^{-4} J/in^2. This value is an order of magnitude greater than the 63.4 µJ/in^2 reported in [4]. The difference can be attributed to the fact that Charipar measured the energy as a gradient from 0 to 80

dc volts with a measured capacitance rather than and AC driving voltage. This would result in a lower energy consumption in Charipar's reported result which confirms that our result is reasonable. As a result, the energy reported in the model should be a more accurate representation of the energy required to drive the pixel. In addition, differences can be attributed to imperfections in the display as well as inaccurate values for resistivity and dielectric constants which can be revised with testing and further research. It should be noted that the hydrophobic layer used in Charipar et al. was different from the layer used in our design. Because of the nature of the pixel stack, this could have a sizable impact on the simulation results and should be kept in mind when interpreting the results. Despite these differences, we do feel that the model is a decent approximation of the display and can be finetuned in the future to more closely reflect empirical values.

Model Weaknesses

To ensure that the model was a general representation of the display, the model proposed does not consider the effects of having many pixels in an array. The effect of including multiple pixels would force the model to consider the edge fields of the electrodes, which would likely have a negligible effect in the macroscopic scale, however this was not the intent of the model, and is therefore not considered.

In addition to not supporting an array of pixels, this model only considers the power consumed when switching from the covered state to the uncovered state. The model can be improved to include these values by simply extending a similar thought process to the channel electrodes and reporting two values for consumed power in switch.

MATLAB Model Results

The MATLAB model was used to generate an approximation of what the voltage across at the top of the pixel layer (under the oil) would be. Using this value, we were able to determine the current and the total energy consumed by the pixel, as well as the time it took to turn from a dark to a light pixel. Again, this model is dependent on the oil vacating the pixel in an exponential in proportion to the energy added to the entire device. However, since we were not able to determine this value through our lab work, this constant (alpha in our model) was approximated to be the slowest possible switch given the findings in [4].

Effect of Actuation Voltage on Energy and Switching Time

In our model, when we varied the initial excitation amplitude, we were able to obtain the relationship between that amplitude and the time & energy required for a switch. These two relationships are graphed below over a span of 10 V to 150 V amplitude.

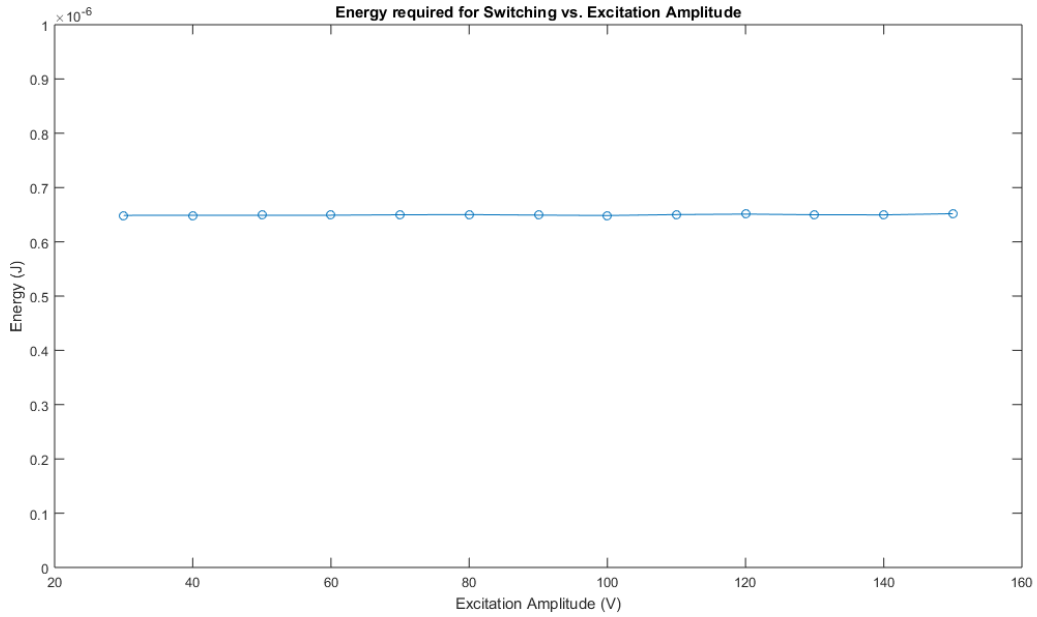

Figure 16. Energy required for switching vs. excitation voltage

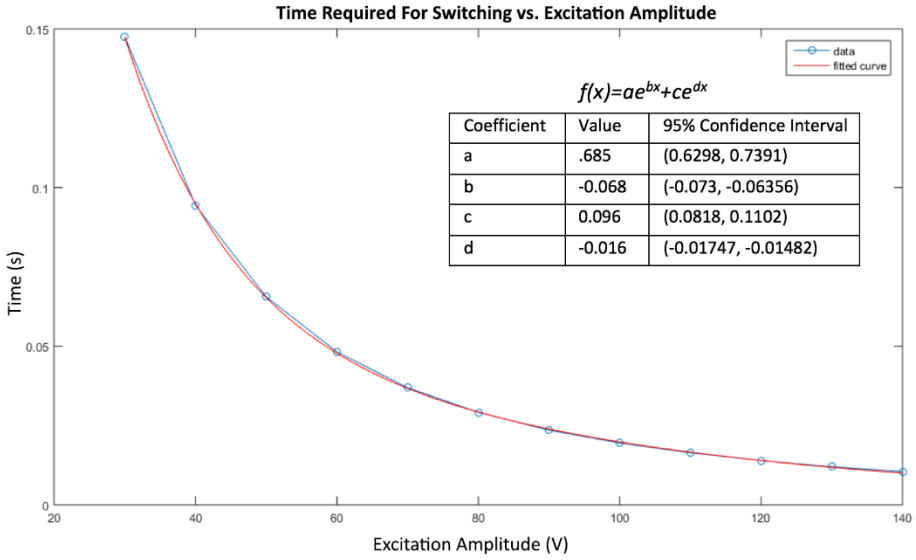

Figure 17. Time required for switching vs. excitation voltage

From these images, we can observe that the higher voltage indeed does reduce the overall time required for a switch, but the energy required for a change approximately stays the same. This suggests that for the designer of such a device, the voltage

requirements are mostly determined by the time required to switch. We fit the switching time to the excitation amplitude using a two-term exponential fit shown next to Figure 16.

Effect of Alpha Constant (Hydrophobicity and Quality) on Energy and Switching Time

We varied the alpha constant in the model within its order of magnitude as a generic and qualitative measure of the quality of the device and the effectiveness of the hydrophobic layer. A device whose pixel surface is very rough or has aberrations would have a slower time to change from dark to light due to the extra energy required for the liquid to overcome the rough surface and vacate the surface. This suggests that a lower alpha constant would lead to a slower change and higher energy required. This was confirmed by the model, which showed that both the switching time and the switching energy is closely fit by a two-term decaying exponential trend. The fits are shown below.

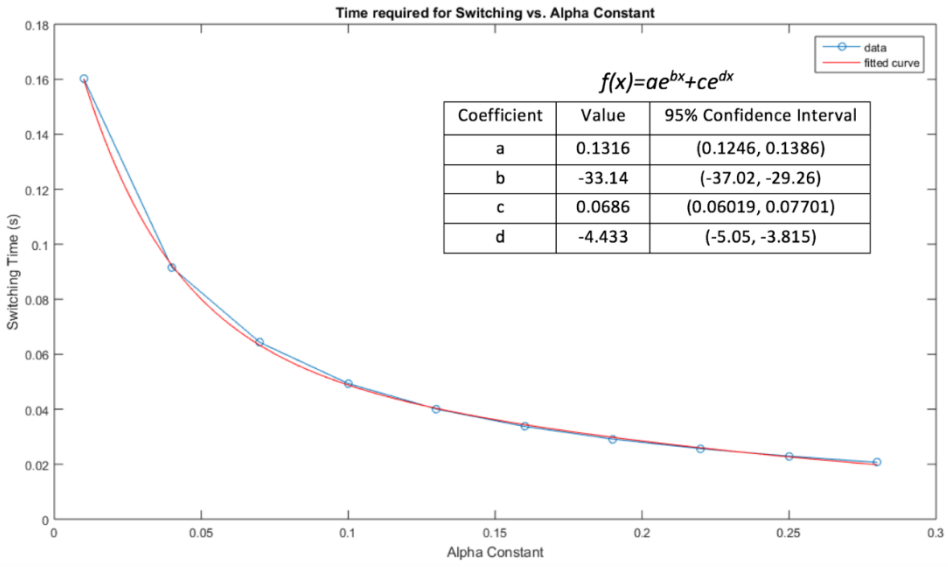

Figure 18. Time Required for Switching vs. Alpha Constant

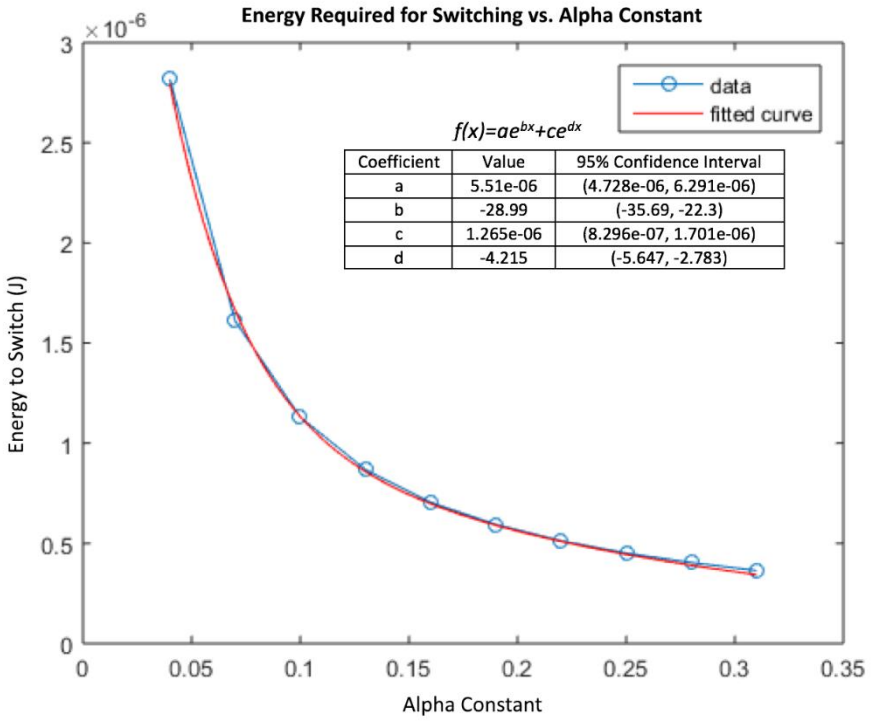

Figure 19. Energy Required for Switching vs. Alpha Constant

Effect of Pixel Size on Energy and Switching Time

We also used the model to assess the relationship between pixel scale and the time and energy required to switch. We essentially scaled the pixel size in the display but not the channel size, which overall leads to less oil covering the pixel. There is a slight possibility a pixel that is too big would not be sufficiently covered by the oil in the channel, but we ignore that possibility for now.

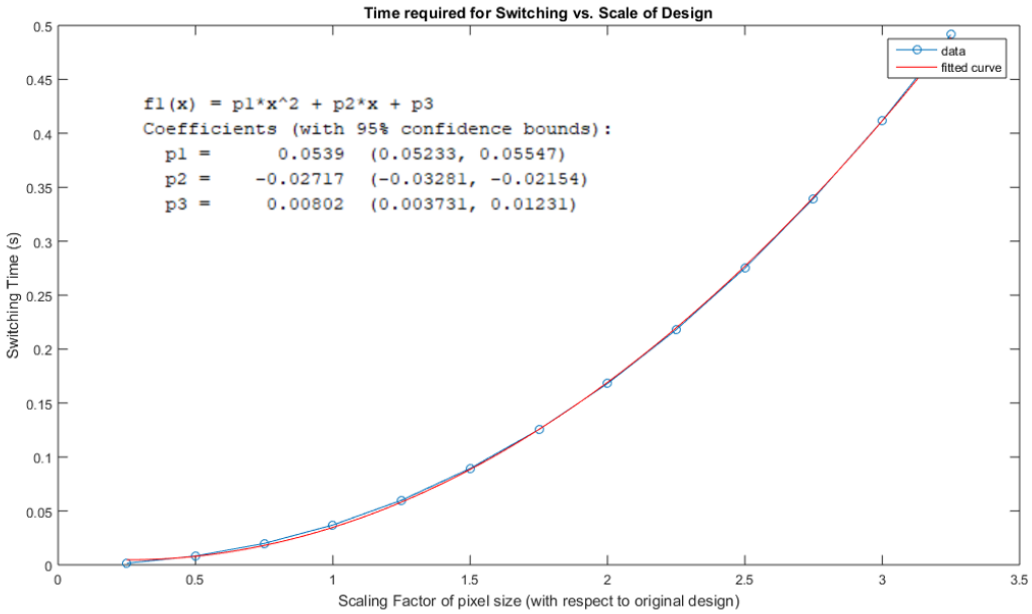

Figure 20: Time Required for Switching vs Pixel Size

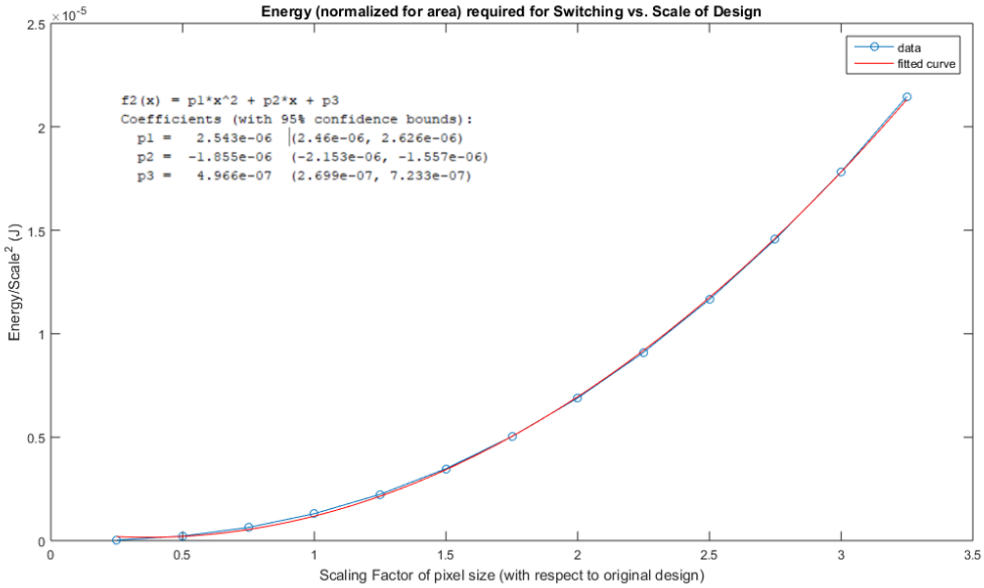

Figure 21: Energy Required for Switching vs Pixel Size

As can be seen, the scaling of the pixel size leads to an parabolic growth in both the energy required as well as the time required for switching. The smaller the pixel, the

better the power consumption per pixel. However, this might not scale for a very dense pixel array, and smaller pixels do require more expensive lithography and etching techniques.

Model Weaknesses

The main weakness in this model is its simplicity. The real device stack contains many more components than just the oil and the pixel. The impact of the hydrophobic layer is neglected in this model. Additionally, a major drawback in this model is that there is not an easy way to estimate how quickly the oil will vacate the top of the pixel. Tang et al. used fluid dynamics principles and the Stokes equations to predict the movement of the oil, and used COMSOL to validate their results [35]. A purely circuit-based model that tries to incorporate the moving oil without the proper constants will not solve this problem. Additionally, we use a parallel-plate capacitor approximation which might not be entirely appropriate across a large display with many pixels. Finally, [4] suggests that the capacitance of the system changes over time, which would affect the total energy values as well.

Discussion

Remarks on MATLAB Model

Of the variables tested using the MATLAB model, the ones that stand out in terms of design of large-scale displays are the pixel size and the actuation voltage. The result that we found was that, bigger pixels lead to more power consumption per area, and that actuation voltage has a limited effect on the overall energy consumption per switch because less time is needed to move the oil. This implies that high amounts of voltage can be used on the device in order to achieve a high switching speed without endangering the power draw of the device. That being said, the actuation voltage is obviously limited in a product-oriented scope by the breakdown voltages of the various materials. A higher voltage generally would imply a higher risk of failures that lead to a low deice longevity, such as the electrolysis of the oil, dielectric breakdown of the SU-8, and charge trapping. The second conclusion about the power consumption scaling exponentially with pixel scale is also an important result. This implies that only small pixels should be used.

The major change from our model versus the previous literature is that our power consumption is much higher than what was presented in [4]. The literature value of 63.4 $\mu J/in^2$ is significantly lower than our models' values, which were 790 $\mu J/in^2$ for the CircuitLab model and ~2100 $\mu J/in^2$ for the MATLAB model. If we assume this is the energy required for a 36ms switch on average, this gives us an equivalent values of 3.4014 mW/cm^2 and 9.0417 mW/cm^2. This discrepancy can be explained through the fact that the energy measurement in [4] was done by measuring the capacitance of the device

at static DC voltages, which was then integrated from 0 to 80 V to give a "switching energy" (where 80 V is the switching voltage). Additionally, the leakage voltage implied a much higher resistance than what we calculated for unknown reasons. Our models do not use DC voltage, they use AC voltage at 10 KHz and measure the energy as a measure of voltage multiplied by actuation time. This driving voltage is closer to what an actual device actuation would look like, since DC voltage might cause charge trapping. This explains the discrepancy in the two values and suggests that our values are more accurate.

That being said, a power that is less than 10 mW/cm^2 still ranks very well among the display devices that were shown in [29]. The figure from that publication is reproduced here. As can be seen, many values less than 10 mW/cm^2 is better than PM-OLED, AM-OLED, certain types of thin film transistors (TFTs), and TFELs.

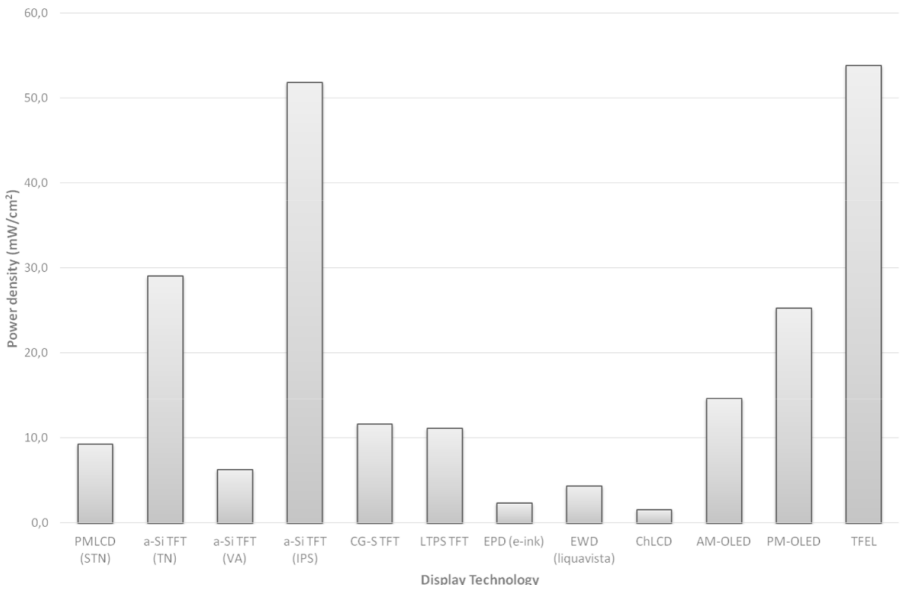

Figure 2, reproduced for convenience. Taken from [29].

Recommendations for Large-Scale Electrowetting Displays

Super pixels

Our research demonstrates that translating the proposed electrowetted display into a large-scale display, such as those that might eventually replace billboards and be used in e-wallpaper applications, presents a few problems. The primary problem being that larger pixels which are more common in digital billboards because they conserve display connections, also require *exponentially* more power to actuate and break down at large enough sizes. The natural solution to this is to group pixels into "super pixels" which would be actuated on the same signal, conserving connections. In addition, "super pixel" power consumption would only increase *linearly* as a function of the number of pixels in the "super pixel", which would decrease the amount of energy required to actuate a pixel of its size. An additional benefit of using "super pixels" on a large-scale display is that individual pixel failure would not aversely affect the display quality, as many smaller, adjacent pixels are also in the same state.

Our recommendation for how to implement "super pixels" in a large-scale display is to identify a critical "sub pixel" size by weighing desired manufacturing cost against desired energy consumption and pixel size feasibility. Once a "sub pixel" size has been identified, a desired resolution can be specified, which will dictate the number of "sub pixels" in a "super pixel."

Manufacturing

The commercial viability of any proposed EWD is contingent upon the mass-manufacturability of the design. Each step of the fabrication process must correspond to a known method of production for semiconductor devices. While the methods used by the

team in creating the screen components are useful for testing and rapid prototyping, they are not sufficient for mass production as it took one person to manually manufacture each individual screen component.

Creating the raised pixel structures and etching the ITO electrodes are the two most important steps to the mass fabrication process. We have been given informal suggestions that soft stamping is the best method to create the pixels, especially because they are regular and rectangular. This is a well-established process that has been shown to work well for fabricating raised structures on top of glass substrates [37]. The material that would be used for the pixels will need to be different as well, because SU-8 is primarily a prototyping material that is quite expensive. Clear polymers and glass-like substances would be appropriate for this purpose.

The ITO electrodes can be formed through plasma etching [38]. Plasma etching or other high-precision etching methods would be much more robust than our current method of timed soaks. Another suggestion would be to deposit the ITO using vapor deposition [39]. This would be especially preferable because of the difficulties that we encountered with etching ITO, which often gave unreliable results. Additionally, the hydrophobic layer is perhaps best depositing using vapor deposition as well or dip-coating [40]. Dip-coating is an effective method in the laboratory for an even film, but the uniformity of dip-coating on our uneven surface with the channels is a cause of concern that would need to be explored. Overall, the robustness of these techniques has not been tested for this particular design, and further experimentation would be required to get an adequate estimate of device lifetimes.

Future Research Directions

This research can be extended by in filling in the simple simulations with data from other sources. These main sources would include COMSOL simulations to better assess the accuracy of our “alpha” constant and the overall model of the oil moving off the pixel. This is of utmost importance because the rupture voltage theory that was presented in [35] and [36] make the assumption that the oil is pinned to the ends of the pixel. While the same idea of rupture voltages might be applied to our model, the fact that the oil is not pinned to the sides of the pixel and will instead fall into the challenges suggests a different calculation of the rupture voltage that must be investigation. Additionally, the models could be better supplemented with data from actual fabricated models.

This would inform us on a question that this research leaves us with, which is to assess how passive matrix would affect the longevity of this device. Passive matrixing requires that a pixel be actuated using both the top and bottom electrode. However, even when a given pixel is not being targeted for actuation, either the top or the bottom electrode (but not both) might still have a voltage at any given time. While 80 V might be used to switch a pixel using two rails of -40V and 40V, every pixel might still experience 40V even when it is not being targeted for actuation because another pixel in the same row or column is being targeted. So, the question of whether or not 40V would cause any oil to move is still an open question. This problem is complicated by the problems with calculating an accurate rupture voltage as mentioned above.

Another open question is that we are still unsure of how the charge on this device distributes itself to create the non-linear capacitance profile that was found in [4]. The

way that charge pinning or surface tension keeps the oil constrained on top of the pixel or within the channel remains to be investigated in a more theoretical fashion in order to bring rigor as to why the device functions in the way that it does. Theoretical rigor in terms of how the surface tension is affected at the corners as well as how the charges rearrange to change the surface tension values might lead to better understandings of what variations in the design could give better results. Mainly, materials, pixel shapes, and surface impurities might be better examined if we had a physical model.

Overall, continued research into the theoretical aspects of this device design in conjunction with lab work to measure variables in our models would allow us to create better models. Combining this with an iterative design process would result in a better evaluation of the various aspects of the Charipar et al. [4] design such as materials and dimensions, and how those aspects could be changed to achieve a better, low-power bistable display that is viable for manufacturing on a wide scale.

Appendix A: Electrical Property Constants

- Single ITO Layers: 50 uΩ, N/A F
- SU-8 Dielectric: 259 TΩ, 391.4 fF
- Fluoropel Hydrophobic Layer: 444 TΩ, 190 fF
- Oil: 232GΩ, 1.036 pF
- Saline Solution: 574Ω, 4.39 pF

Appendix B: MATLAB Simulation Code

```
sweepx = [];
sweepy = [];
sweepz = [];
sweepa = [];
for sweep = .25:.25:4

    % Channel widths
    channel_width = 100 * 10^-6;
    pixel_size1 = 300 * 10^-6 * sweep;
    pixel_size2 = 900 * 10^-6 * sweep;
    pixel_depth = 22 * 10^-6;
    dielectric_depth = 3 * 10^-6;

    total_pixel_area_per_pixel = pixel_size1 * pixel_size2;
    total_channel_area_per_pixel = ((pixel_size1 + pixel_size2) *  ...
        channel_width + 4 * (channel_width/2)^2);

    oil_volume = total_channel_area_per_pixel * pixel_depth;
    height_of_oil = oil_volume / total_pixel_area_per_pixel;
    % Resistances and Capacitances
    SU8_dielectric_constant = 4.1;
    SU8_resistivity = 2.8*10^16 * (10^-2);
    channel_su8_resistance = SU8_resistivity * (dielectric_depth) ...
        / total_channel_area_per_pixel;
    pixel_su8_resistance = SU8_resistivity * (dielectric_depth +
pixel_depth) ...
        / total_pixel_area_per_pixel;

    channel_su8_capacitance = total_channel_area_per_pixel * 8.84*10^-
12 * ...
        SU8_dielectric_constant / (dielectric_depth);
    pixel_su8_capacitance = total_pixel_area_per_pixel * 8.84*10^-12 *
...
        SU8_dielectric_constant / (dielectric_depth + pixel_depth);

    oil_dielectric_constant = 4.6;   % dodecanol, cant find resistance
so will just put a high value
    oil_resistivity = 1/(3.5 * 10^-10);
    channel_oil_capacitance = total_channel_area_per_pixel * 8.84*10^-
12 * ...
        oil_dielectric_constant / (pixel_depth);
    pixel_oil_capacitance = total_pixel_area_per_pixel * 8.84*10^-12 *
...
        oil_dielectric_constant / (height_of_oil);
    channel_oil_resistance = oil_resistivity * (height_of_oil) ...
        / total_channel_area_per_pixel;
    pixel_oil_resistance = oil_resistivity * (pixel_depth) ...
        / total_pixel_area_per_pixel;

    % FOR THE PIXEL

    rsolid = pixel_su8_resistance;
```

```
    roil = pixel_oil_resistance;
    csolid = pixel_su8_capacitance;
    coil = pixel_oil_capacitance;

    % Build Equation
    syms t y(t)
    A = 80 * sin(t*2*pi*10000);
    dAdt = matlabFunction(diff(A, t));
    mask = @(t) .5*square(t*pi, 25)+.5;
    A = matlabFunction(A);
    Amask = @(t) A(t) .* mask(t);
    dAdtmask =  @(t) dAdt(t) .* mask(t);
    alpha = -log(.22) / ((-22/sqrt(2))^2 * .036); % which is going to a
ratio of 4.5:1 in 36 ms as it said in Charipar that it would.
    myode = @(t, y) [((Amask(t)./rsolid) - y(1).*(rsolid^-1 + roil^-1)
+ csolid.*dAdtmask(t)) ./ (csolid + coil);
       alpha*-1* y(1).^2 * y(2)];
    tspan = 0:.00001:.5;
    starting_volume_normalized = 1*(oil_volume)/(2.8600e-12);
    [x, y] = ode45(myode, tspan, [0 starting_volume_normalized]);

    diffV = myode(x, y);
    Ioil_capacitance = (coil) * diffV(1:50001);
    Ioil_resistance = y(:,1) / roil;
    signal_voltage = A(tspan)';
    pixel_voltage = signal_voltage - y(:,1);
    total_I = Ioil_capacitance(1:50001) + Ioil_resistance;
    Ipixel_resistance = pixel_voltage / rsolid;
    Ipixel_capacitance = total_I - Ipixel_resistance;
    power = abs((Ioil_capacitance + Ioil_resistance) .* y(1:50001,1));
    power = power + abs((Ipixel_resistance + Ipixel_capacitance) .*
pixel_voltage);

    index_when_hits_contrast = find(y(:,2) < .22, 1);
    time = tspan(index_when_hits_contrast);
    time_span = tspan(2) - tspan(1)
    energy = sum(power(1:index_when_hits_contrast) * time_span);

    sweepx = [sweepx, sweep]
    sweepy = [sweepy, time]
    sweepz = [sweepz, energy]
    sweepa = [sweepa, energy/(sweep^2)]

end
figure(1)
f1 = fit(sweepx(1:13)', sweepy(1:13)', 'poly2')
plot(f1, sweepx(1:13), sweepy(1:13), '-o')
xlabel('Scaling Factor of pixel size (with respect to original
design)')
ylabel('Switching Time (s)')
title('Time required for Switching vs. Scale of Design')
figure(2)
f2 = fit(sweepx(1:13)', sweepa(1:13)', 'poly2')
plot(f2, sweepx(1:13), sweepa(1:13), '-o')
xlabel('Scaling Factor of pixel size (with respect to original
design)')
```

```
ylabel('Energy/Scale^2 (J)')
title('Energy (normalized for area) required for Switching vs. Scale of
Design')
```

References

[1] J. Rawert, D. Jerosch, K. Blankenbach, and F. Bartels, “15.2: Bistable D3 Electrowetting Display Products and Applications,” *SID Symposium Digest of Technical Papers*, vol. 41, no. 1, pp. 199–202, May 2010.

[2] B. J. Feenstra *et al.*, “Electrowetting-Based Displays: Bringing Microfluidics Alive On-Screen,” in *19th IEEE International Conference on Micro Electro Mechanical Systems*, 2006, pp. 48–53.

[3] “All Modes of Operation - Liquavista - Electrowetting based low power, always viewable color video displays.” [Online]. Available: http://www.liquavista.com/technology/electrowetting-benefits/all-modes-of-operation/. [Accessed: 07-Nov-2016].

[4] K. M. Charipar, N. A. Charipar, J. V. Bellemare, J. E. Peak, and A. Piqué, “Electrowetting Displays Utilizing Bistable, Multi-Color Pixels Via Laser Processing,” *Journal of Display Technology*, vol. 11, no. 2, pp. 175–182, Feb. 2015.

[5] Miortech, *Etulipa’s revolutionary display technology can lift the ban on digital billboards.* 2013.

[6] K. H. Kang, “How Electrostatic Fields Change Contact Angle in Electrowetting,” *Langmuir*, vol. 18, no. 26, pp. 10318–10322, Dec. 2002.

[7] Y.-P. Zhao and Y. Wang, “Fundamentals and Applications of Electrowetting,” *Reviews of Adhesion and Adhesives*, vol. 1, no. 1, pp. 114–174, Feb. 2013.

[8] J. Ignacio Polanco, *Liquid, Isolator, Substrate*. 2013.

[9] “(PDF) micromachines Dynamics of Electrowetting Droplet Motion in Digital Microfluidics Systems: From Dynamic Saturation to Device Physics,” *ResearchGate*. [Online]. Available: https://www.researchgate.net/publication/278687418_micromachines_Dynamics_of_Electrowetting_Droplet_Motion_in_Digital_Microfluidics_Systems_From_Dynamic_Saturation_to_Device_Physics. [Accessed: 29-Apr-2019].

[10] M. Abdelgawad and A. R. Wheeler, “Low-cost, rapid-prototyping of digital microfluidics devices,” *Microfluid Nanofluid*, vol. 4, no. 4, p. 349, Jul. 2007.

[11] “What is Electrowetting? - Liquavista - Electrowetting based low power, always viewable color video displays.” [Online]. Available: http://www.liquavista.com/technology/what-is-electrowetting/. [Accessed: 09-Oct-2016].

[12] B. J. Feenstra and R. A. Hayes, “Video-speed electronic paper based on electrowetting,” *Nature*, vol. 425, no. 6956, pp. 383–385, Sep. 2003.

[13] H. You and A. J. Steckl, “Three-color electrowetting display device for electronic paper,” *Applied Physics Letters*, vol. 97, no. 2, p. 023514, Jul. 2010.

[14] A. J. Steckl and H. You, “Lightweight electrowetting display on ultra-thin glass substrate,” *Jnl Soc Info Display*, vol. 21, no. 5, pp. 192–197, May 2013.

[15] M. Chen, X. Liang, W. Hu, L. Zhang, C. Zhang, and H. Yang, “A polymer microsphere-filled cholesteric-liquid crystal film with bistable electro-optical characteristics,” *Materials & Design*, vol. 157, pp. 151–158, 2018.

[16] G. W. Jones and A. P. Ghosh, “Passive matrix OLED display,” May 2000.

[17] M. Oomura, “Active matrix display,” Feb. 2004.

[18] M. Riahi, K. A. Brakke, E. Alizadeh, and H. Shahroosvand, “Fabrication and characterization of an electrowetting display based on the wetting–dewetting in a cubic structure,” *Optik - International Journal for Light and Electron Optics*, vol. 127, no. 5, pp. 2703–2707, Mar. 2016.
[19] J. Feenstra and R. Hayes, “Electrowetting Displays.” Liquivista BV, May-2009.
[20] P. Sureshkumar and S. S. Bhattacharyya, “Display Applications of Electrowetting,” *Journal of Adhesion Science and Technology*, vol. 26, no. 12–17, pp. 1947–1963, Sep. 2012.
[21] A. L. Dalisa, “Electrophoretic display technology,” *IEEE Transactions on Electron Devices*, vol. 24, no. 7, pp. 827–834, Jul. 1977.
[22] J. Shinar and V. Savvateev, “Introduction to Organic Light-Emitting Devices,” in *Organic Light-Emitting Devices*, J. Shinar, Ed. Springer New York, 2004, pp. 1–41.
[23] S. Writer, “Demystifying OLED Displays For Digital Signage,” *Sixteen:Nine*, 25-Apr-2016. .
[24] “U.S. Digital Signage Market Size, Analysis | Industry Report, 2018-2025,” Oct-2018. [Online]. Available: https://www.grandviewresearch.com/industry-analysis/us-digital-signage-market. [Accessed: 19-Apr-2019].
[25] “Samsung The Wall MicroLED and 85-inch QLED TV | First Look Video,” *Digital Trends*, 07-Jan-2018. [Online]. Available: https://www.digitaltrends.com/home-theater/samung-microled-tv-and-85-inch-qled-tv-first-look/. [Accessed: 19-Apr-2019].
[26] B. Demory, K. Chung, A. Katcher, J. Sui, H. Deng, and P.-C. Ku, “Integrated parabolic nanolenses on MicroLED color pixels,” *Nanotechnology*, vol. 29, no. 16, p. 165201, Feb. 2018.
[27] V. W. Lee, N. Twu, and I. Kymissis, “Micro-LED Technologies and Applications,” *Information Display*, vol. 32, no. 6, pp. 16–23, 2016.
[28] S. Dash, “MicroLED: Emerging as a Next Generation Display Technology,” *DisplayDaily*, 08-Apr-2019. [Online]. Available: https://www.displaydaily.com/article/display-daily/microled-emerging-as-next-generation-display-technology. [Accessed: 19-Apr-2019].
[29] M. R. Fernández, E. Z. Casanova, and I. G. Alonso, “Review of Display Technologies Focusing on Power Consumption,” *Sustainability*, vol. 7, no. 8, pp. 10854–10875, Aug. 2015.
[30] A. Industries, “ITO (Indium Tin Oxide) Coated Glass - 50mm x 50mm.” [Online]. Available: https://www.adafruit.com/product/1310. [Accessed: 01-Apr-2019].
[31] MicroChem, “S1800_Photoresist.pdf,” *MicroChem Corp.* [Online]. Available: http://microchem.com/products/images/uploads/S1800_Photoresist.pdf. [Accessed: 02-Apr-2019].
[32] “SU-8 3000 :: MicroChem.” [Online]. Available: http://microchem.com/Prod-SU83000.htm. [Accessed: 01-Apr-2019].
[33] “SU-8 2000 :: MicroChem.” [Online]. Available: http://www.microchem.com/Prod-SU82000.htm. [Accessed: 01-Apr-2019].
[34] “Droplet Actuation by Electrowetting-on-Dielectric (EWOD): A Review: Journal of Adhesion Science and Technology: Vol 26, No 12-17.” [Online]. Available: https://www.tandfonline.com/doi/abs/10.1163/156856111X599562. [Accessed: 02-Apr-2019].

[35] B. Tang, J. Groenewold, M. Zhou, R. A. Hayes, and G. (G F.) Zhou, “Interfacial electrofluidics in confined systems,” *Scientific Reports*, vol. 6, p. 26593, May 2016.
[36] Q. Zhao *et al.*, “Electrowetting on dielectric: experimental and model study of oil conductivity on rupture voltage,” *J. Phys. D: Appl. Phys.*, vol. 51, no. 19, p. 195102, Apr. 2018.
[37] S. Kuo and C. Lin, “Non-Spherical SU-8 Microlens Array Fabricated Utilizing a Novel Stamping Process and an Electro-Static Pulling Method,” in *2009 IEEE 22nd International Conference on Micro Electro Mechanical Systems*, 2009, pp. 987–990.
[38] M. Mohri, H. Kakinuma, M. Sakamoto, and H. Sawai, “Plasma Etching of ITO Thin Films Using a CH4/H2 Gas Mixture,” *Jpn. J. Appl. Phys.*, vol. 29, no. 10A, p. L1932, Oct. 1990.
[39] “Continuous, Highly Flexible, and Transparent Graphene Films by Chemical Vapor Deposition for Organic Photovoltaics - ACS Nano (ACS Publications).” [Online]. Available: https://pubs.acs.org/doi/abs/10.1021/nn901587x. [Accessed: 29-Apr-2019].
[40] D. Grosso, “How to exploit the full potential of the dip-coating process to better control film formation,” *Journal of Materials Chemistry*, vol. 21, no. 43, pp. 17033–17038, 2011.